Case Studies in Construction Materials 11 (2019) e00293

Contents lists available at ScienceDirect

Case Studies in Construction Materials

journal homepage: www.elsevier.com/locate/cscm

Case study

Performance evaluation of cashew nutshell ash as a binder in concrete production

Solomon Oyebisi[a,*], Tobit Igba[b], David Oniyide[b]

[a] Department of Civil Engineering, Covenant University, Ota, Nigeria
[b] Department of Civil Engineering, Federal University of Agriculture, Abeokuta, Nigeria

ARTICLE INFO

Article history:
Received 18 June 2019
Received in revised form 11 October 2019
Accepted 14 October 2019

Keywords:
Cashew nutshell ash
Reactivity indexes
Compacting factor
Compressive strength
Split tensile strength
Pozzolanic material

ABSTRACT

The agro-industrial sector annually produces large volumes of waste by-products which as a result of the ignorance of their values as well as their ineffective management, pose environmental, societal and economic threats. Thus, this study explored the ash from cashew nutshell waste and replaced it with Portland limestone cement (PLC) at 5%, 10%, 15% and 20% using a mix design ratio of grade 25 MPa concrete (M 25). The cashew nutshell was sun-dried for 14 days and then burnt in a gas furnace at a temperature of 750 °C for 5 h to obtain cashew nutshell ash (CNSA). The chemical and physical properties of the CNSA were examined while the workability of the fresh concrete was investigated. Moreover, the mechanical and durability properties of the hardened concrete were carried out while the microstructures of the concrete samples were analyzed. The experimental findings revealed that CNSA met the requirements for use as a pozzolanic material. The slump and the compacting factor increased with increasing CNSA content. Moreover, both compressive, splitting tensile and flexural strengths of the hardened concrete increased as the content of CNSA increased but optimum at 15% replacement level. Furthermore, the CNSA concrete resisted more sulfate attack than the Portland cement concrete (control). The micromorphological analysis exhibited a reticular structure and adequate filling ability with the incorporation of CNSA content in the mix. Hence, it is recommended that CNSA can be incorporated as a construction material in the concrete production at the optimum replacement with PLC at 15% for structural application and 20% for non-load bearing application. This study is advantageous because fresh concrete would remain workable for longer periods, thus, resulting in the reduction of construction joints. Moreover, the utilization of CNSA concrete is also beneficial in an environment with high sulfate content. Finally, the developed model equations from this study can be used in the development of mix design of blended concrete as well as a better refinement of existing procedure of concrete mix design provided the chemical composition of the materials is established.

1. Introduction

Concrete is a versatile construction product which comprises cement, aggregates, water and sometimes admixtures to influence its fresh or hardened properties. The Portland limestone cement (PLC) reacts with water to form a paste and bind the aggregates. Cement plays the role of a binder in concrete. It is a substance that sets, hardens and binds

* Corresponding author at: Department of Civil Engineering, Covenant University, P.M.B. 1023, Km 10, Idiroko Road, Ota, Ogun State, Nigeria.
E-mail address: solomon.oyebisi@covenantuniversity.edu.ng (S. Oyebisi).

https://doi.org/10.1016/j.cscm.2019.e00293

alternative materials. Portland limestone cement is widely used and it is the second-largest material after water used as a construction material in the construction industry but its production emits carbon dioxide (CO_2) to the atmosphere [1]. However, the growing initiatives and awareness for environmental preservation and conservation of natural resources with the aim to reduce the CO_2 emission through the impact of PLC production by the 2030 agenda for Sustainable Development Goals cannot be overstressed [2]. Consequently, the agro-industrial wastes, otherwise known as supplementary cementitious materials (SCMs) such as fly ash, ground granulated blast furnace slag, corncob ash, and rice husk ash have been widely utilized to partially and completely replace PLC in the production of concrete [3–14]. Thus, the environmental and economic threats of PLC can be reduced through the use of agro-industrial wastes that are pozzolanic in nature.

Pozzolanic materials are materials which comprised mostly oxides of silica and alumina, and little cementitious value which chemically react with $Ca(OH)_2$ in finely divided form in the presence of moisture at ordinary temperature to form compound possessing cementitious properties [1,15–19]. However, pozzolan cannot exhibit pozzolanic and or hydraulic reactivity in the absence of hydrated lime. Hence, hydrated lime (such as PLC) is needed to release and activate it during its hydration as a binding agent [20–26]. The reactivity of any pozzolan is generally quantified by its silica content and essentially governed by its fineness, chemical composition, mineralogical composition and specific surface area [27–32]. Thus, the evaluation of pozzolanic reactivity of any pozzolan is required in the blended cement. In the same vein, Xie and Visintin [16], Xie and Ozbakkaloglu [17], Sakai, Miyahara, Ohsawa, Lee and Daimon [18] and Alp et al. [19] stated that the reactivity of various blended binders cannot be evaluated by any single index. Therefore, it is recommended that a single index, either reactivity modulus (RM), hydraulic modulus (HM) or lime modulus (LM) can be used to evaluate hydraulic reactions, while both silica modulus (SM) and alumina modulus (AM) are needed to evaluate the pozzolanic reactions [16,16,17,18,19]. Furthermore, during the process of hydration, a pozzolanic reaction occurs between the reaction of a Portlandite ($Ca(OH)_2$) and the reactive silica. This reaction results in the additional formation of C-S-H with binding properties [33]. Therefore, pozzolanic materials have widely gained an acceptance in the construction industry in some countries as binding agents to improve the properties of both fresh and hardened concretes in building construction, and to stabilize soil [24,25,34].

Cashew (*Anacardium occidentale*) is a cash crop, found and produced in Nigeria, India, Brazil, Vietnam, and Central America. According to the Food and Agriculture Organization of the United Nations [35], the yearly production of cashew nuts in Nigeria is estimated to be 636,000 metric tons (MT). However, most processing industries generate a cashew nutshell as a waste by-product and indiscriminately dispose or burn it [36,37]. In essence, Cashew nutshell is an agricultural waste and it serves as a major means of land and environmental pollution in areas where it is been cultivated or processed but not utilized. The CNSA represents approximately 5% of the initial weight of cashew nut. Until now, there is few or no research on the utilization of CSNA as construction material in civil engineering practice. Pandi and Ganesan [38] studied the water absorption and sorptivity of PC concrete partially replaced with CNSA. It was discovered that PC concrete showed lower water absorption and sorptivity at 25% replacement by CNSA than conventional concrete. In a related study, Pandi et al. [39] investigated the optimum utilization of CNSA in concrete production. The findings revealed that 25% replacement of PC by CNSA resisted more axial and bending loads and permeability than conventional concrete. Moreover, Thirumurugan et al. [40] examined the strength property of concrete partially replaced with CNSA. The results revealed that a 20% replacement of PLC by CNSA increased the concrete strength with a water-cement ratio of 0.45. In the same vein, Pandi and Ganesan [41] investigated the sorptivity and water absorption of mortar incorporated with CNSA. It was found that the water absorption of CNSA mortar with 1:3 mix was higher than convectional mortar, while the sorptivity was lower than conventional mortar. However, Lima et al. [42] examined the physical and chemical analysis of CNSA as a cement composite. The results of chemical tests showed that the CNSA contained a low content of silicon oxide (SiO_2) and this restricted its utilization as a pozzolanic material in blended cement.

This study, therefore, filled a gap by harnessing the potential of using CNSA from another source as a pozzolanic material and replacing it with PLC in the production of concrete. The study also adopted the concept of reactivity indexes through the chemical and mineralogical compositions of both PLC and CNSA, and the mix design proportion to develop a model for the prediction of mechanical properties of concrete blended with CNSA. In addition, the durability of the concrete through immersion in a sulfate solution was investigated. The experimental findings were compared with the control mix (Portland cement concrete (PCC)) and the recommendations made. The harness and utilization of CNSA in the construction sector would reduce the construction cost, extenuate the environmental, technical and economic threats posed by the production of PLC, reduce the solid waste, thereby driving sustainability as well as improving concrete properties. Moreover, the predictions from this study would reliably and significantly improve the mix design proportion of concrete blended with CNSA by reducing the need to perform multiple-trial tests.

2. Materials and methods

2.1. Materials

Dangote 3X grade 42.5 R PLC was obtained and utilized to satisfy the specifications of the Nigerian Industrial Standard [43]. The Portland cement concrete (PCC) served as a control mix. Three different samples of cashew nutshell as shown in Fig. 1 were collected from the cashew processing unit of the Federal University of Agriculture, Abeokuta. The shell was the

Fig. 1. (a) Cashew nutshell (CNS) (b) burning of CNS in a gas furnace and (c) CNSA.

waste product of the cashew seed and it was obtained after the nut has been removed. The cashew nutshell was sun-dried for seven days to aid the burning process and then burnt in a gas furnace at a temperature of 750 ^{0}C for 5 h to obtain cashew nutshell ash (CNSA) as shown in Fig.1. The ash was sieved with BS sieve size 45 μm to obtain a fine particle similar to PLC. The physical properties of binders used (PLC and CNSA) are presented in Table 1. Moreover, the oxide compositions of CNSA, PLC and various mix proportions of blended binders were analyzed at the University of Ibadan, Ibadan, Nigeria with the aid of x-ray fluorescence (XRF) spectrophotometer machine, Philips PW-1800.

The binders' fineness was determined in consonance with the procedures stipulated by BS EN [44]. The dry sieving method was adopted. A 100 g of each binder was accurately weighed and placed on a BS 90 μm sieve. The sample was continuously sieved for 15 min. The residue left after 15 min was weighed and the fineness of the binders was obtained in accordance with Eqn. 1(a) and the result is shown in Table 1.

$$W_r = \frac{W_S}{W_t} \tag{1a}$$

where Wris the weight of residue (fineness) (in %)

WSis the weight of specimen retained on the sieve (in g)

Wtis the weight of the specimen (in g)

The Blaine method as prescribed by BS EN [44] was used to determine the specific surface area of the binders. The air did not pass through the bed at a constant rate but a known content of air passed at a stipulated average pressure. The time at which the flow took place was measured, and for a given standard porosity of 0.500, the specific surface area was determined and the result is presented in Table 1.

The specific gravity of binders (PLC and CNSA) was also determined in consonance with BS EN [44]. A pycnometer of 100 ml was used, freed from moisture content, and thoroughly dried. The weight of the empty pycnometer was measured and recorded as W_1. Thereafter, a 50 g of the binder was weighed and put in the pycnometer. The weight of the pycnometer with sample and stopper was measured and noted as W_2. Moreover, kerosene was poured in the sample up to the neck of the pycnometer, thoroughly mixed, and ensured that no air bubbles left in the bottle. The weight of the pycnometer with sample and kerosene was measured and recorded as W_3. Finally, the pycnometer was emptied and filled with kerosene up to the tip of the bottle, and the weight was determined and noted as W_4. Thus, the specific gravity (Sg) of the binder was calculated in accordance with Eqn. 1(b). The results are presented in Table 1.

$$Sg = \frac{W_1 - W_2}{(W_1 - W_2) - (W_3 - W_4)} \tag{1b}$$

The aggregates, fine aggregate (FA) and coarse aggregate (CA) used were obtained from Alabata, Abeokuta, Nigeria. They were prepared and used in conformity with the British Standard (BS) EN [45]. Water for the mixing and production process

Table 1
Physical properties of binders used.

Property	CNSA 1	CNSA 2	CNSA 3	Average CNSA	PLC
Specific gravity	3.12	3.10	3.08	3.10	3.15
Specific surface area (m^2/kg)	580	600	634	605	350
Fineness (%)	2.00	1.92	1.93	1.95	3.57

was obtained from the Civil Engineering laboratory of the Federal University of Agriculture, Abeokuta, Nigeria, and conformed to the BS [46]. All tests were conducted in the laboratory at a temperature of 25–28 ^{0}C and relative humidity of 60–65%. In determining the specific gravity of aggregate, a 2 kg of aggregate was weighed, thoroughly washed to remove fines and dust, drained, placed in the wire basket and the whole content was immersed in the potable water at a temperature of 27 ^{0}C with 50 mm cover of water above the top of the basket for 24 h. The content was then transferred to the second dry cloths, allowed to dry for 60 min in an air-tight container and weighed. Finally, the aggregate was transferred to a shallow tray and placed in an oven at a temperature of 110 ^{0}C for 24 h. It was then removed from the oven, cooled in an air-tight container and weighed [. Thus, the result was obtained according to Eq. 2. The results are presented in Table 1.

$$Sg = \frac{W_1 - W_2}{(W_1 - W_2) - (W_3 - W_4)} \tag{2}$$

where Sg is the specific gravity of the aggregateW_1 is the weight of oven-dried aggregate in the air (in g)W_2 is the weight of saturated surface dried aggregate in the air (in g)W_3 is the weight of saturated aggregate + basket suspended in water (in g) $W_4$is the weight of basket suspended in water (in g)

The water absorption capacity of aggregates was determined in accordance with the methods stated by BS EN [45] and as earlier explained for the specific gravity. Hence, the result was obtained according to Eqn.3 and the result is presented in Table 2.

$$W_a = \frac{W_S - W_O}{W_O} \times 100 \tag{3}$$

where W_a is the water absorption capacity as a per cent of dry weight (in %)W_S is the weight of saturated surface dry aggregates in the air (in g)W_O is the weight of oven-dried aggregate in the air (in g)

The moisture content of aggregates was also determined in accordance with the methods stated by BS EN [45]. A clean container with its lid was properly dried and weighed. A 2 kg of aggregate was accurately weighed and placed in the container with the aid of scoop. The lid was replaced and the whole content was weighed. Thereafter, the lid was removed while the container and the test sample was placed in the oven and dried at a temperature of 105 ^{0}C for 24 h. Afterward, the whole content was removed from the oven, placed in an air-tight container and allowed to cool for 45 min. Finally, the lid was replaced and the whole content was weighed. Thus, the result of the moisture content was obtained according to Eqn. 4 and shown in Table 2.

$$M_C = \frac{W_{CW} - W_{CD}}{W_{CD} - W_C} \times 100 \tag{4}$$

where M_C is the moisture content as a percentage of dry weight (in %)W_{CW} is the weight of the container + lid + weight of wet aggregate (in g)W_{CD} is the weight of the container + lid + weight of dry aggregate (in g)W_C is the weight of dry container + lid (in g)

2.2. Reactivity indexes of binders

The reactivity indexes (RI) of both CNSA and PLC were quantified using the major reactive oxides which are CaO, SiO_2, Al_2O_3, Fe_2O_3, MgO, and SO_3 from the chemical composition of the binders (CNSA and PLC) to reflect their hydraulic and pozzolanic reactivity [16–19,47]. The reactivity indexes are illustrated with Eqs. 5–9 as reactivity modulus (RM), hydraulic modulus (HM), lime modulus (LM), silica modulus (SM) and alumina modulus (AM) respectively [16,19–24,47]. The hydraulic/cementitious properties were evaluated by RM, HM, and LM, while the pozzolanic properties were evaluated by both SM and AM [16,19,20,47–49].

$$RM = \frac{CaO + MgO + Al_2O_3}{SiO_2} \tag{5}$$

$$HM = \frac{CaO}{SiO_2 + Al_2O_3 + Fe_2O_3} \tag{6}$$

Table 2
Physical properties of aggregates used.

Property	FA	CA
Specific gravity	2.60	2.69
Fineness modulus	2.62	2.93
Water absorption (%)	0.65	0.80
Moisture content (%)	0.32	0.22
Surface structure	sharp	smooth
Particle shape	round	round

$$LM = \frac{1.0CaO - 0.7SO_3}{2.8SiO_2 + 1.1Al_2O_3 + 0.7Fe_2O_3} \quad (7)$$

$$SM = \frac{SiO_2}{Al_2O_3 + Fe_2O_3} \quad (8)$$

$$AM = \frac{Al_2O_3}{Fe_2O_3} \quad (9)$$

2.3. Concrete mix design proportion

The concrete mix proportion was designed in consonance with the procedures stipulated in the BS EN [50] and the results of the mix proportions and identifications for grade 25 MPa concrete (M 25) are shown in Table 3. In the course of mix design, the physical properties of the materials such as specific gravity, water absorption, and moisture content were put into consideration to have a standardized mix design for the selected ratio. The mix ID A (100% PLC + 0% CNSA) was prepared as a control sample.

2.4. Mixing, casting, sample preparation, and curing

The manual method was adopted for the concrete mix. The PLC was replaced with CNSA at 0%, 5%, 10%, 15% and 20% as a result of previous studies that 20–25% replacement of PLC by CNSA exhibited the optimum mechanical strength [38–40]. The aggregates and the binders (PLC and CNSA) were mixed thoroughly in a dry state for about 5 min; water was then added in a gradual manner and continued mixing for additional 5 min to attain the mixing homogeneity. The fresh concrete was then filled into the 150 mm standard cubical and 100 mm cylindrical concrete moulds in two and three layers respectively and compacted on a hard level surface with a 16 mm standard rod. Thereafter, the concrete cubes and cylinders were removed from the moulds after 24 h and submerged in the water curing tank under the ambient conditions (25-28 ^{0}C and 60% ± 5% RH) till the testing days, 7, 14, 28 and 90 days. Three specimens were made for each test.

2.5. Experimental tests and analysis

2.5.1. Workability test

The slump and the compacting factor tests of the fresh concrete samples were carried out in consonance with the procedures stipulated by the BS EN [51,52] respectively. The slump cone mould was filled with fresh concrete in three equal layers and compacted with 35 strokes of tamping rod. Thereafter, the mould was vertically lifted upward and the difference in height of the collapsed concrete with respect to the height of the slump cone was measured and recorded. Moreover, for the compacting factor test, the fresh concrete was gently placed in the upper hopper to its brim with the aid of scoop. The surface of the mould was leveled and the cylinder was covered while the trap door of the lower hopper was opened to allow fresh concrete to fall into the cylinder below. Afterward, the cylinder with the fresh concrete was weighed and recorded as a partially compacted concrete. Moreover, the cylinder was emptied and then refilled with the same concrete mix in 50 mm deep layers, and each layer was heavily compacted to obtain a fully compacted concrete. The top surface of the cylinder was leveled and the fully compacted concrete was weighed and recorded. Finally, the empty cylinder was weighed and recorded, and the result of the compacting factor value was obtained.

2.5.2. Mechanical test

The compressive, splitting tensile and flexural strengths tests on the hardened concrete samples were conducted based on the procedures stated by the BS EN [53–55] respectively. The sizes of the cube, cylinder, and beam used were 150 mm, 150 mm by 300 mm long, and 150 mm by 600 mm long respectively. The axial load was applied to the hardened concrete

Table 3
Mix design quantity for M 25.

Mix ID	Mix Proportion	PLC (kg/m^3)	CNSA (kg/m^3)	FA (kg/m^3)	CA (kg/m^3)	Water (kg/m^3)
A	100% PLC + 0% CNSA	340	0	715	1035	210
B	95% PLC + 5% CNSA	323	17	715	1035	210
C	90% PLC + 10% CNSA	306	34	715	1035	210
D	85% PLC + 15% CNSA	289	51	715	1035	210
E	80% PLC + 20% CNSA	272	68	715	1035	210

samples until the failure occurred and the compressive, splitting tensile and flexural strengths were obtained based on Eqs. 10–12 respectively.

$$fc = \frac{F}{A} \tag{10}$$

where fc is the compressive strength (in MPa) F is the applied load on 150 mm cube at failure (in N) A is the cross-sectional area of the sample (in mm^2)

$$fct = \frac{2P}{\pi dl} \tag{11}$$

where fct is the splitting tensile strength (in MPa)P is the applied load at failure (in N) l is the length (300 mm) of the concrete specimen (in mm)d is the diameter (150 mm) of the concrete sample (in mm)

$$fr = \frac{1.5Pl}{bd^2} \tag{12}$$

where fr is the flexural strength (in MPa) P is the applied load at failure (in N) l is the distance between the support rollers (in mm) b is the width (150 mm) of the concrete sample (in mm) d is the depth (150 mm) of the concrete sample (in mm)

2.5.3. Durability test

The sulfate resistance test of the hardened concrete was carried out in consonance with the BS EN [56]. The concrete samples were immersed in 5% $MgSO_4$ solution for 90 days and tested for weight and strength losses. The magnesium sulphate ($MgSO_4$) solution was selected because extensive physical deterioration was more witnessed when a concrete sample is immersed in $MgSO_4$ than in sodium sulphate (Na_2SO_4) solution [1,57,58]. The microstructures of the selected samples were examined at the University of Ibadan, Ibadan, Nigeria using a scanning electron microscopy (SEM) instrument, Model JEOL-70006000.

2.5.4. Prediction of compressive strength

One of the reactivity indexes (RIs), RM, HM or LM was used to signify the strength of hydraulic/cementitious reactivity of the blended binders, and both SM and AM were used to indicate the strength of pozzolanic reactivity in consonance with the previous studies (16, 19, 20, 47–49). Consequently, the compressive strength of hardened concrete samples was correlated with the RI of each mix design proportion using the fit regression model in Minitab 17 statistical software. Compressive strength (f_c) was selected as response and the RIs were selected as continuous predictors. The correlation between the f_c and the RI were analyzed using Eqs. 13–15 as the combination of RM, SM and AM; HM, SM, and AM; and LM, SM and AM respectively, and the best fit regression model was selected.

$$f_c = \beta + \alpha_1 RM + \alpha_2 SM + \alpha_3 AM \tag{13}$$

$$f_c = \beta + \alpha_1 HM + \alpha_2 SM + \alpha_3 AM \tag{14}$$

$$f_c = \beta + \alpha_1 LM + \alpha_2 SM + \alpha_3 AM \tag{15}$$

where f_c is the compressive strength (in MPa) RM is the reactivity modulus of the blended binders HM is the hydraulic modulus of the blended binders LM is the lime modulus of the blended binders SM is the silica modulus of the blended binders AM is the alumina modulus of the blended binders β, α_1, α_2, α_3 are the magnitudes of coefficients

The compressive strength (f_c) of hardened concrete is directly proportional to the RI of the blended binders and inversely proportional to the water-cement (w/b) ratio of the mix design proportion [16]. Thus, the f_c of concrete was also examined based on the function of RI and w/b ratio using Eqs. 16–18 as the combination of RM, SM, AM and w/b ratio; HM, SM, AM and w/b ratio; and LM, SM, AM and w/b ratio respectively.

$$f_c = \beta + \left(\frac{\alpha_1 RM + \alpha_2 SM + \alpha_3 AM}{w/_b}\right) \tag{16}$$

$$f_c = \beta + \left(\frac{\alpha_1 HM + \alpha_2 SM + \alpha_3 AM}{w/_b}\right) \tag{17}$$

$$f_c = \beta + \left(\frac{\alpha_1 LM + \alpha_2 SM + \alpha_3 AM}{w/_b}\right) \tag{18}$$

The binder-aggregate (b/agg) ratio (in volume fraction) according to Xie and Visintin [16], Geisenhansluke and Schmidt [59] and Sebaibi, Benzerzour, Sebaibi and Abriak [60] played a vital factor apart from the RI and w/b ratio in determining and controlling the mechanical strength of hardened concrete. Therefore, the study also modeled the correlation between the f_c and the combination of RI, w/b ratio and b/agg ratio using the Eqs. 19–21 as the combination of RM, SM, AM, w/b ratio and b/agg ratio; HM, SM, AM, w/b ratio and b/agg ratio; and LM, SM, AM, w/b ratio and b/agg ratio respectively.

$$f_c = \beta + \left(\frac{\alpha_1 RM + \alpha_2 SM + \alpha_3 AM}{w/_b}\right)\left(b/_{agg}\right) \tag{19}$$

$$f_c = \beta + \left(\frac{\alpha_1 HM + \alpha_2 SM + \alpha_3 AM}{w/_b}\right)\left(b/_{agg}\right) \tag{20}$$

$$f_c = \beta + \left(\frac{\alpha_1 LM + \alpha_2 SM + \alpha_3 AM}{w/_b}\right)\left(b/_{agg}\right) \tag{21}$$

3. Result and discussions

3.1. Oxide compositions of binders

The results of oxide compositions of CNSA as presented in Table 4 indicated that the CNSA met the chemical pozzolanic requirements stated by the BS EN [61], ASTM [62] and BS EN [63] in that the addition of silica (SiO_2), alumina (Al_2O_3) and ferric oxide (Fe_2O_3) met the minimum requirement of 70%. The LOI's requirements of ASTM [62] of less than 5% and BS EN [61], BS EN [63] and BS EN [64] of less than 10% were also fulfilled. However, the requirements stated by Al-Akhras [65] for the pozzolanic and cementitious nature of lime (CaO) content between 10% and 20% were not met. In addition, the chemical moduli of ($CaO + MgO/SiO_2$) above 1 and (CaO/SiO_2) of less than or equal to 1.4 for cementitious materials stated by BS EN [63] and BS EN [66] were not fulfilled. Moreover, the addition of SiO_2, CaO, and MgO of greater than or equal to 67% by BS EN [66] for a cementitious material was not met. On the other hand, a conclusion that CNSA could exhibit pozzolanic reactivity can be inferred because the BS EN [63]'s requirement of a silica content of 25% minimum was met. Comparing the oxide content of CNSA used with the content obtained in the previous studies, the silica content of the CNSA used exhibited a similar silica content with XRF results of Pandi and Ganesan [38], Pandi et al. [39], Thirmurugan et al. [40], and Pandi and Ganesan [41] whose silica (SiO_2) revealed a 62.85%, 62.85%, 54.85% and 62.85% respectively, and this resulted in their inference that CNSA could be used as a Pozzolanic material. However, the XRF results of CNSA by Lima et al. [42] showed a silica content of 12.17% and this, according to the study, restricted its utilization as a pozzolanic material in blended cement. Owing to these previous studies and the relevant standards, the CNSA used in this study has proved to be a pozzolanic material and can be utilized as a binder in concrete production for structural and non-load bearing applications. In addition, the PLC fulfilled the requirements of BS EN [64].

3.2. Reactivity indexes of binders

The reactivity index (RI) of the binders (CNSA and PLC) are illustrated in Fig. 2. Owing to the high content of lime (CaO, 64.5%) in PLC and very low content of lime (0.86%) in CNSA, the results of RM, HM and LM were 3.32, 2.14 and 0.92 for PLC and 0.27, 0.01 and 0.001 for CNSA respectively. Statistically, there is an increase of 91.87%, 99.53% and 99.89% in RM, HM and LM for PLC when compared with CNSA respectively. Thus, the results inferred that PLC exhibited hydraulic property in that they satisfied the requirements of BS EN [66] with the optimal values of both RM and HM above 1, and the requirements of BS EN

Table 4
Oxide compositions of binders used.

Oxide Composition (%)	CNSA 1	CNSA 2	CNSA 3	Average CNSA	BS EN 450-1 [61] Requirements for Pozzolan	PLC	BS EN 196-2 [64] Requirements for PLC
CaO	0.80	1.02	0.76	0.86	–	64.5	61 - 69
SiO_2	63.87	64.15	63.83	63.95	$SiO_2 + Al_2O_3 + Fe_2O_3 = 70\%$ min	21.55	18 – 24
Al_2O_3	14.94	14.98	14.93	14.95		5.50	2.6 – 8.0
Fe_2O_3	12.46	12.62	12.44	12.51		3.08	1.5 – 7.0
MgO	1.53	1.54	1.52	1.53	4.0 max	1.52	0.5 – 4.0
K_2O	0.51	0.40	0.56	0.49	–	0.62	0.2 -1.0
Na_2O	0.34	0.32	0.36	0.34	5.0 max	0.14	–
SO_3	1.03	0.85	1.01	0.96	3.0 max	1.12	0.2 – 4.0
LOI	2.55	2.28	3.12	2.65	10.0 max	1.28	5.0 max

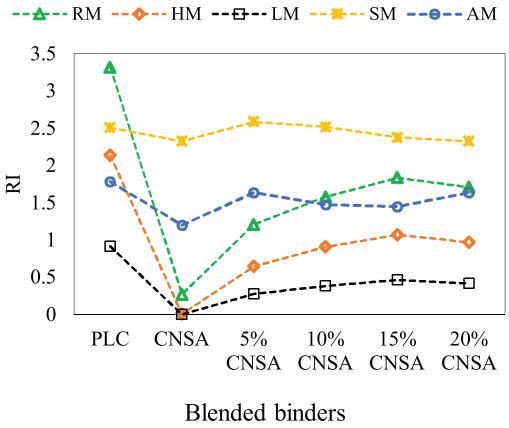

Fig. 2. Reactivity indexes of blended binders.

[63] with the optimal value of LM of greater than or equal to 0.60 and less than or equal to 1.02. The results also supported the findings of Xia and Visintin [16], Xie and Ozbakkaloglu [17], and Sakai et al. [18] that PLC, due to its high lime content, exhibits the RM, HM, and LM with a value greater than 1. On the other hand, CNSA exhibited an SM of 2.33 and AM of 1.20 due to the high content of silicate and aluminate in the material. This affirmed the findings of Xia and Visintin [16], Xie and Ozbakkaloglu [17], and Sakai et al. [18] that SCMs possessed a higher content of silica and alumina and this resulted in high SM and AM when compared with the corresponding RM, HM, and LM. Therefore, it is inferred that CNSA is supplementary silica and alumina source for pozzolanic reactivity and this supported the previous studies that a pozzolanic material of a natural origin with a low content of magnesia (MgO) and sulfate (SO_3) but with the addition of a high content of alumina and silica of greater than 75% resulted in a high pozzolanic reactivity [67,68]. Furthermore, it is noteworthy to establish from the XRF of blended binders as shown in Fig. 3 that both CaO and SO_3 decreased with increasing CNSA content. However, SiO_2, Al_2O_3, Fe_2O_3, and MgO increased with increasing CNSA content. This supported the previous studies that in the cement blends, CaO and SO_3 decrease with the increase in pozzolan content while SiO_2, Al_2O_3, Fe_2O_3 and MgO increase with the increase in pozzolan content [19,69]. Consequently, the RM, HM, and LM of the PLC blends from Fig. 2 decreased with increasing CNSA content and maintaining a gradual increase from 5 to 15% replacement level. In addition, the SM increased with increasing CNSA content up to 10% replacement level.

3.3. Workability

The results of the slump and the compacting factor tests are shown in Fig. 4. It was noticed from Fig. 4 that the slump and the compacting factor of the concrete mixes increased with increasing CNSA content. The slump increased from 30 to 75 mm while the compacting factor increased from 0.845 to 0.885 as the CNSA increased from 0 to 20%. These results may be attributed to the specific surface area of the CNSA which is higher than that of PLC. Also, the particle shape of pozzolan (CNSA) contributed to the increased rate of workability [1]. Moreover, the result was in line with the behavior of other established pozzolanic materials such as corncob ash, pulverized fly ash, metakaolin, rice husk ash which have been affirmed to enhance the workability of fresh concrete due to their lower specific gravities and densities which increase the mix

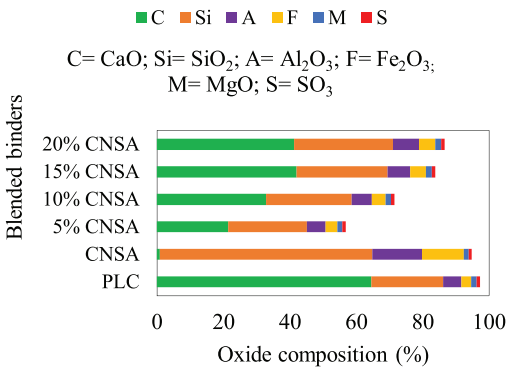

Fig. 3. XRF results of blended binders.

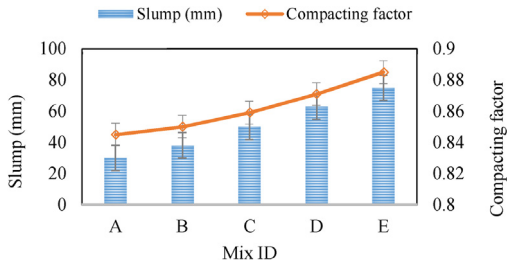

Fig. 4. Slump and compacting factor values.

volume, reduce the friction between the binding particles and enhance a better flow of fresh concrete [5,6]. However, the result from this study was contrary to the findings of Pandi et al. [39] which established that the slump of cement concrete blended with CNSA decreased with increasing CNSA content. This may be as a result of the high content of CaO (35.67%) which influences the hydraulic properties, resulting in quick setting, hardening and strengthening properties of the blended binder [16], comparing to a very low content of CaO (0.86%) of the CNSA used in this study. On the other hand, a conclusion that CNSA could manifest a workable and cohesive mix can be deduced because the BS EN [51,52]'s maximum specifications

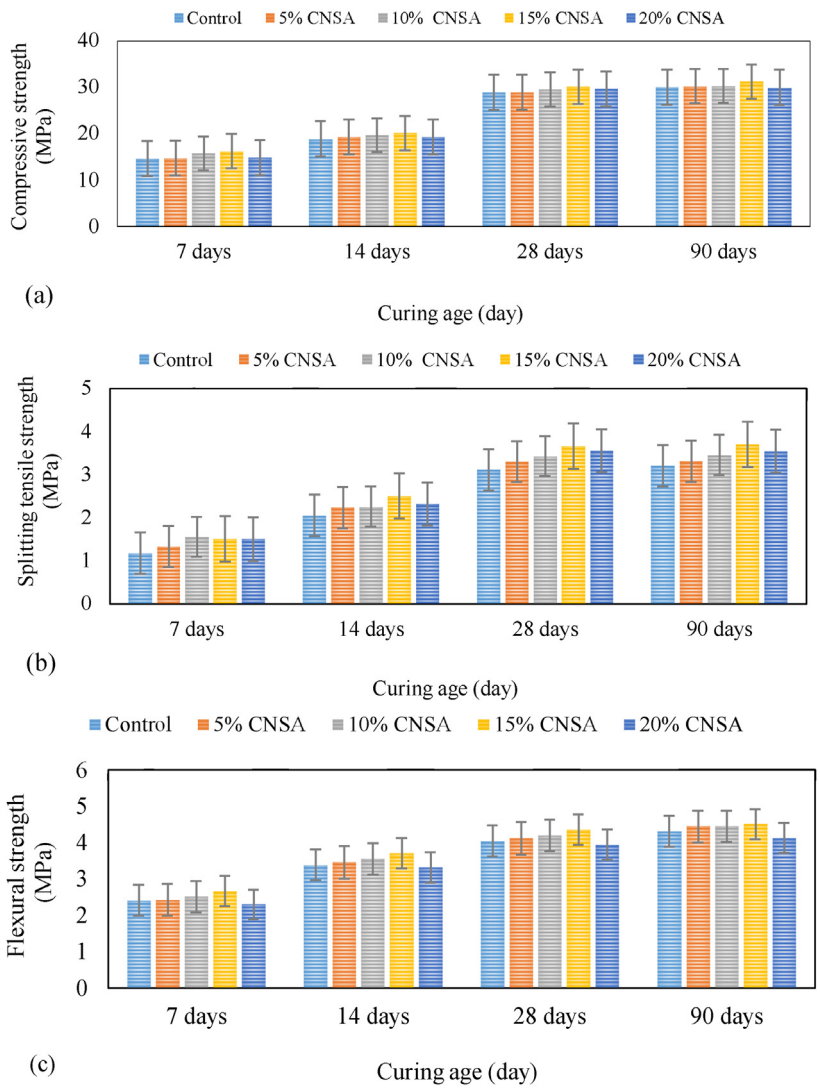

Fig. 5. Mechanical properties (a) compressive (b) splitting tensile and (c) flexural strengths.

of both slump and compacting factor of 150 mm and 0.950 were met respectively. Therefore, it can be inferred that concrete incorporated with CNSA shows the possibility of using less water to optimize strength in consonance with Abram's law of water-cement-ratio [70].

3.4. Mechanical properties

Fig. 5 (a)–(c) present the results of compressive, splitting tensile and flexural strengths tests as the arithmetic means of the three test cubes, cylinders, and beams for each sample and age respectively. It was revealed that the compressive strength increased with increasing CNSA content from 5 to 15% replacement level at all curing ages when compared with the control (PCC). This increase in strength when compared with the control sample can be attributed to filler effect of the CNSA in the blended mix [71,72] and more reactive presence of alkalis and portlandite due to early hydration in the blended mix, promoting the reactivity of CNSA blended cement [73–75]. However, the targeted strength of class M 25 at 28 days of curing was obtained at the 20% replacement level. It was further observed that the compressive strength increased with increasing curing ages, but slightly decreased at 20% replacement level at all curing ages when compared with other concrete mixes. This result was contrary to the findings of Pandi and Ganesan [38], Pandi et al. [39] and Thirumurugan et al. [40] who reported that the compressive strength increased with increasing in CNSA content up to 25% and inferred an optimum replacement level of 25% for structurally applied concrete. This variance may be as a result of chemical and mineralogical compositions of the CNSA [1,15,73,75] in that this study reported a composition of silica (SiO_2), lime (CaO), alumina (Al_2O_3) and ferric oxide (Fe_2O_3) as 63.95%, 0.86%, 14.95%, and 12.51% respectively. But, Pandi and Ganesan [38], Pandi et al. [39] and Thirumurugan et al. [40] reported composition of 62%, 36%, 2.01% and 4.20% for SiO_2, CaO, Al_2O_3, and Fe_2O_3 respectively. Thus, an inference can be made that the CNSA blended concrete is suitable for the structurally applied concrete since it met the specifications of BS EN [53]. On the other hand, the splitting tensile strength increased with increasing CNSA content even up to 20% replacement level at all curing ages. It was also revealed that CNSA-based PCC exhibited more splitting tensile strength than the conventional concrete (PCC). This result affirmed the findings of Pandi et al. [39] who also reported an increase in splitting tensile strength as the CNSA content increased from 5 to 25% replacement level, but at 30% replacement level, the splitting tensile decreased. Thus, it is established that CNSA-based PCC would resist more tensile stress under an applied load than the conventional concrete (PCC). In the same vein, the results of the flexural strength tests also revealed that the strength increased with increasing CNSA content up to 15% replacement level at all curing ages, but at 20% replacement level, the strength reduced. This result also confirmed the findings of Pandi et al. [39] who also reported an increase in flexural strength as the CNSA content increased from 5 to 25% replacement level, but at 30% replacement level, the flexure reduced. Owing to this finding, it can be inferred that the CNSA blended concrete would resist more bending stress under an applied load than PCC.

3.5. Durability property

The effect of sulfate on the weight and strength properties of CNSA blended concrete after 90 days of immersion in 5% $MgSO_4$ is presented in Fig. 6. The illustration from Fig. 6 showed the values of both weight and strength loss as the arithmetic means of the three test cubes for each sample. The differences in percentage weight loss between the specimen cured in water and the other one immersed in $MgSO_4$ solution for 90 days were 10%, 0.87%, 0.89%, 1.83% and 2.38% for the control (PCC), 5% CNSA, 10% CNSA, 15% CNSA and 20% CNSA respectively. Furthermore, it was revealed that the percentage weight loss of the CNSA blended concrete marginally increased with increasing CNSA content. Moreover, it was shown that a concrete blended with CNSA possessed a range of percentage weight loss from 1 to 2.4% as the percentage replacement increased from 5 to 20% when compared with the conventional concrete (PCC) with a percentage weight loss of 10%. On the other hand, the variations in percentage strength loss between the specimen cured in water and the other one immersed in $MgSO_4$ solution for 90 days were 15%, 4.01%, 3.41%, 3.01% and 2.97% for the control (PCC), 5% CNSA, 10% CNSA, 15% CNSA and 20% CNSA respectively. Moreover, it was shown that the percentage strength loss of the CNSA blended concrete marginally decreased with increasing CNSA content. In addition, it was revealed that a concrete blended with CNSA possessed a range of percentage strength loss within 3–4% as the percentage replacement increased from 5 to 20% when compared with the

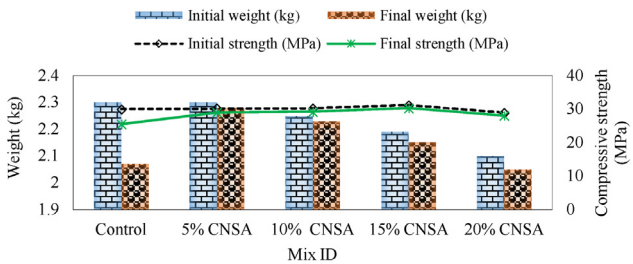

Fig. 6. Sulfate resistance of concrete mixes in 5% $MgSO_4$ solution for 90 days.

conventional concrete (PCC) with a percentage strength loss of 15%. However, a better strength performance of CNSA blended concrete when compared with PCC in the $MgSO_4$ solution from this study was not consistent with the literature in that corncob ash blended concrete and other established SCMs exhibited a lower performance than the conventional concrete in the $MgSO_4$ solution due to little or no $Ca(OH)_2$ and more C-S-H in SCMs which readily reacts with $MgSO_4$ solution and forms a gel of magnesium silicate hydrate (M-S-H) that permits sulfate ions with easy diffusion into the matrix of the concrete [76–78]. Contrarily, during the hydration of cement, the reaction between $Ca(OH)_2$ and $MgSO_4$ solution results in insoluble brucite which prevents the capillary pores and forms an impermeable layer against the diffusion of sulfate ions into the matrix of the concrete [76–78]. Notwithstanding, it can be inferred that CNSA blended concrete resisted more sulfate attack than conventional concrete. These results were consistent with the literature that pozzolanic material refines the pores in the concrete, dilutes the alite (C_3A) and remove the Portlandite ($Ca(OH)_2$) by converting it into a cementitious

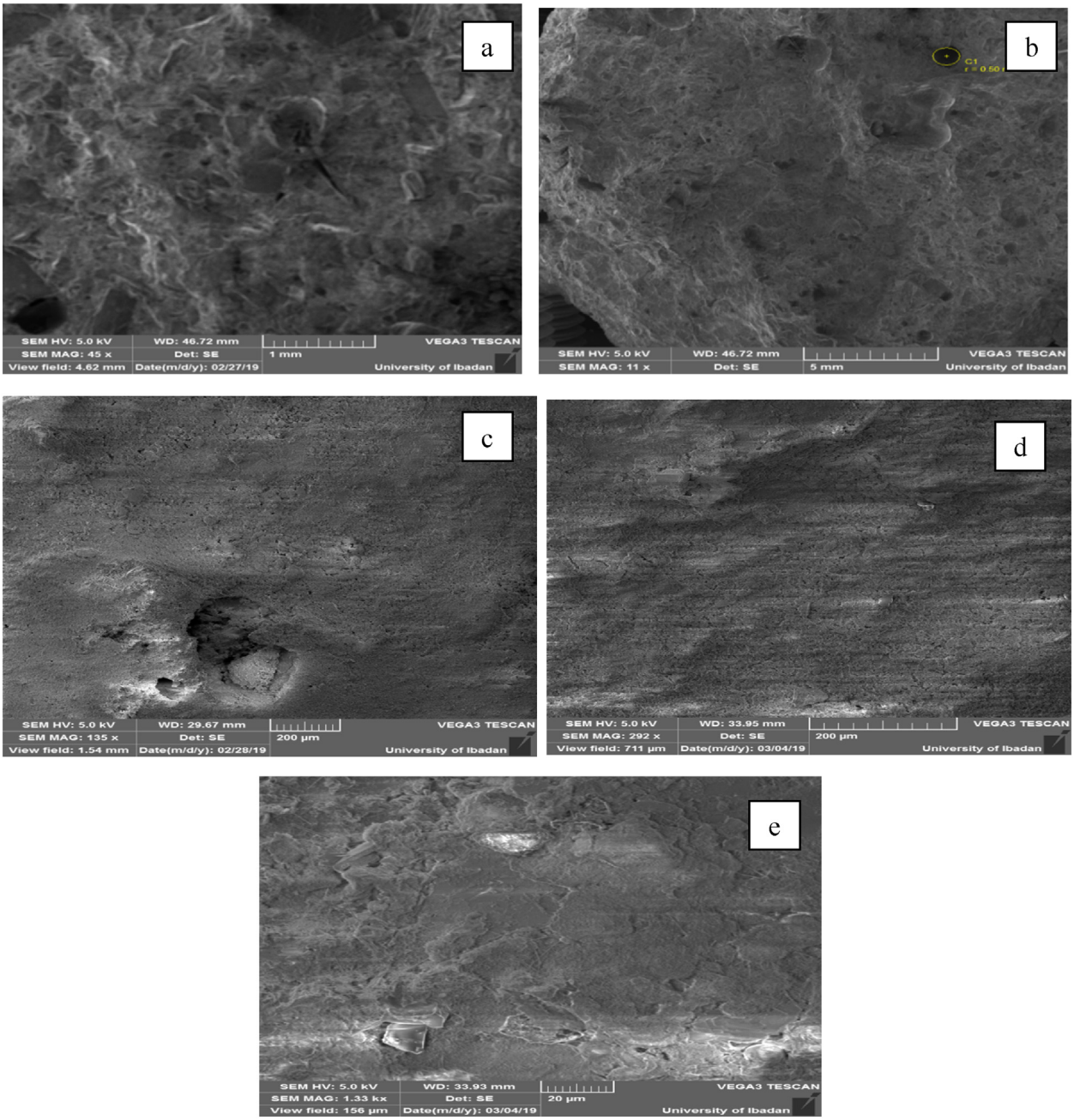

Fig. 7. Micromorphology of mortar specimens cured in water and analyzed after 28 days of hydration on (a) Control, 100% PLC (b) 95% PLC + 5% CNSA (c) 90% PLC + 10% CNSA (d) 85% PLC + 15% CNSA and (e) 80% PLC + 20% CNSA.

material, thereby reducing the formation of gypsum content and resisting the sulfate attack [1,79,80]. However, during the hydration of cement, Portlandite does not precipitate on the grain of cement, but in the voids between the SCMs grains and this attributes to the lower performance of convectional concrete in the $MgSO_4$ solution [81]. In addition, the low content of CaO and the low ratio of SO_3 to Al_2O_3 in the CNSA contributed to the higher sulfate resistance of CNSA blended concrete in the $MgSO_4$ solution when compared with the conventional concrete [82].

3.6. Micromorphological analysis

The micromorphology analysis was conducted on the mortar specimens of the CNSA blended cement to characterize the microstructures at 28 days of hydration at 27 ^{0}C. For the analysis, the working distance and the SEM magnification were 46.72, 46.72, 29.97, 33.93 and 33.95 mm, and 45, 11, 135, 1330 and 292X for the control, 5% CNSA, 10% CNSA, 15% CNSA and 20% CNSA respectively. The SEM voltage was constant at 5.0 kV and the results are presented in Fig. 7.

The SEM micromorphology in Fig. 7(a) showed that the internal structure of the CNSA blended cement mortar revealed good densification and exhibited a wrinkled shape. Moreover, the micromorphology of the specimen showed an adequate compact with a presence of low pores hexagonally flaked with C-S-H gel due to the chemical reaction between the lime (CaO) available in the PLC and the water. Thus, this attribution contributed to the mechanical strength of the hardened product, and consistent with the finding of Bapat [81] that the reaction of lime in cement with water produces a hydrating product of Ca $(OH)_2$ which promotes both early and later age strengths of the hardened product. In the same vein, the micromorphology in Fig. 7(b) to (d) indicated that the internal structure of the specimens was crystalline and reticular in nature. Evidently, the micrograph of the mixes exhibited an adequate compact, uniform matrix, and good densification. It was clearly obvious from the SEM micrographs that the internal pores in the CNSA blended cement mortar reduced with increasing CNSA content due to not only the filler effect of the CNSA on the binding properties but also promotion of a higher gel phase formation [83–86]. The microstructure was reticular with C-S-H gel around the binding powders due to the chemical reaction between the Portlandite ($Ca(OH)_2$) present in the PLC and both silica (SiO_2) and alumina (Al_2O_3) available in the CNSA. This was attributed to the higher mechanical strength of the mortar incorporated with CNSA [86]. In addition, the pores do not significantly contribute to the mechanical strength of the concrete [39,81]. However, the lower mechanical strength reported for 20% CNSA when compared with other mortar mixes as indicated in Fig.7(e) may be attributed to an excess of CNSA content in the mix which slowed the rate of hydration and formation of gel phase of cement mortar, thus, retarding the strength gain [86,87].

3.7. Prediction of compressive strength (Fc)

3.7.1. Prediction of Fc based on reactivity indexes (RI)

The fit regression models which correlate the compressive strength (Fc) based on reactivity indexes (RI) combining RM, SM, and AM; HM, SM, and AM; and LM, SM, and AM are illustrated in Fig. 8 (a), (b) and (c) at 95% confidence interval (CI) respectively. Statistically, it was shown from Fig. 8 (a), (b) and (c) that the coefficients of determination (R^2) were 99.64%,

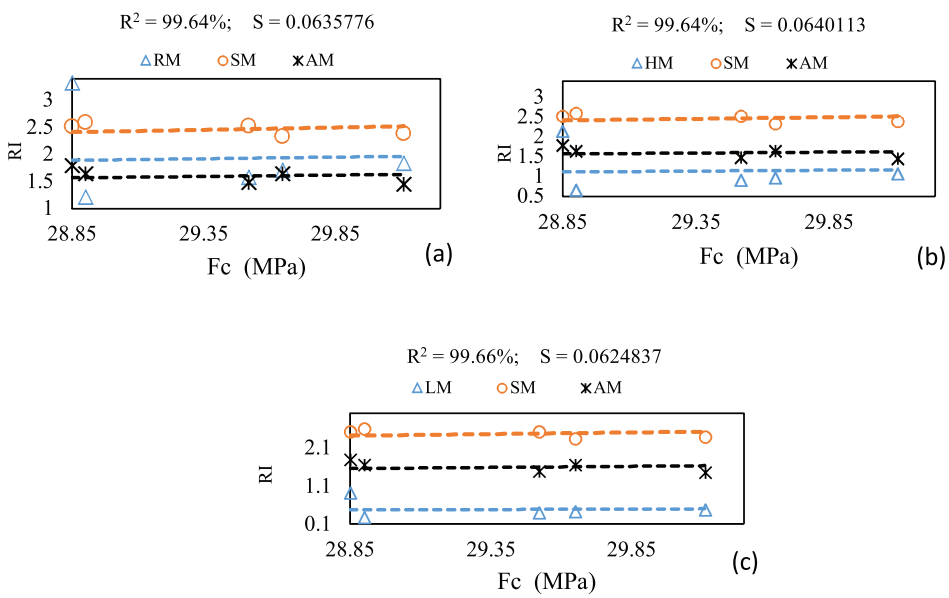

Fig. 8. Fit regression model between Fc and RI.

99.64, and 99.66% significantly fit to correlate the data. Moreover, the combination of LM, S, and AM from Fig. 8(c) yielded the best predictability in that R^2 exhibited the highest value, 99.66%. In addition, the values of standard distance (S) data that fell from the regression line was 0.0624837 because, for a given study, the better the equation predicts the response, the lower S is. However, this assertion was contrary to the findings of Xie and visintin [16] who stated that the combination of RM, SM, and AM yielded the best predictability. The reason may be as a result of the difference in chemical and mineralogical compositions of the blended binders which influence the reactivity and strengthening properties of the final product [1,16,65]. Thus, this study inferred the use of a combination of LM, SM and AM in predicting the relationship between the compressive strength and the reactivity indexes of CNSA blended cement concrete. The fit regression equations for the Fc based on RI for the CNSA blended cement concrete at 28 days of curing for M 25 are illustrated in Eqs. 22–24 for the combination of RM, SM, and AM; HM, S, and AM; and LM, SM and AM respectively.

$$F_C = 40.931 + 0.0791RM - 2.893SM - 2.839AM \tag{22}$$

$$F_C = 40.993 + 0.1108HM - 2.910SM - 2.836AM \tag{23}$$

$$F_C = 40.974 + 0.2590LM - 2.903SM - 2.836AM \tag{24}$$

3.7.2. Prediction of Fc based on RI and water-cement ratio (w/b)

Fig. 9 (a), (b) and (c) showed the fit regression models of Fc based on the RI and w/b for the combination of RM, SM and AM; HM, SM, and AM; and LM, SM and AM respectively. The coefficients of determination (R^2) from Fig. 9 (a), (b) and (c) were 99.64%, 99.64% and 99.66% significantly fit to statistically correlate the data at 95% CI respectively. In comparison, it can be evidently observed that the goodness of fit (R^2 and S) for the prediction of Fc based on RI exhibited the same with the prediction based on RI and w/b. This may be as a result of constant w/b used during the statistical analysis because it has been established that the incorporation of w/b significantly improves the correlation of compressive strength when compared to the use of only RI [16].

The fit regression equations for the Fc based on RI and w/b for the CNSA blended cement concrete at 28 days of curing for M 25 are illustrated in Eqs. 25–27 for the combination of RM, SM, and AM; HM, SM, and AM; and LM, SM and AM respectively. Similarly, the combination of LM, SM, and AM from Fig. 9(c) yielded the best predictability.

$$F_C = 40.931 + \left\{ \frac{0.0489RM - 1.788SM - 1.755AM}{\frac{w}{b}} \right\} \tag{25}$$

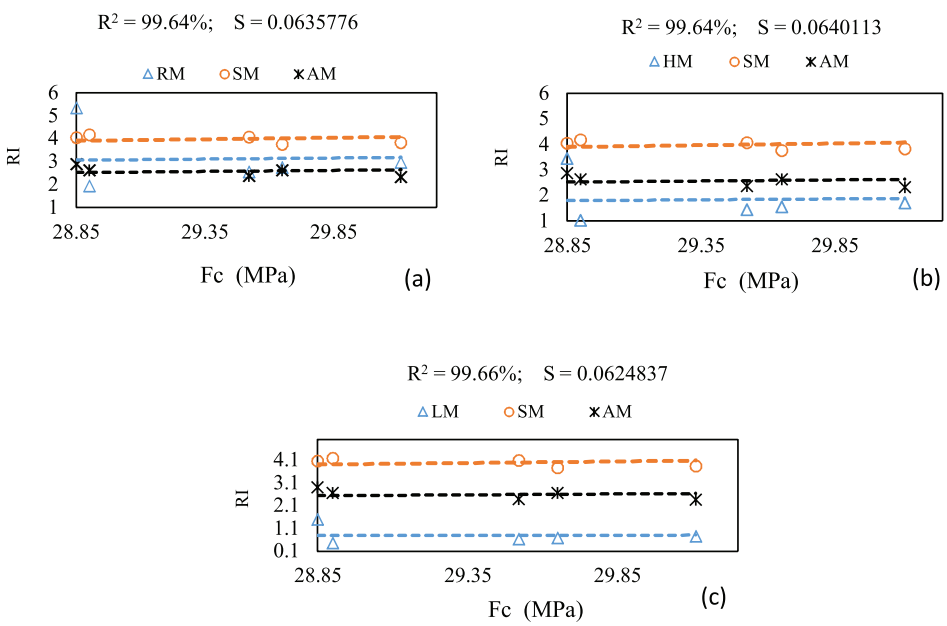

Fig. 9. Fit regression model of Fc based on RI and w/b.

$$F_C = 40.993 + \left\{\frac{0.0685HM - 1.798SM - 1.753AM}{\frac{w}{b}}\right\} \tag{26}$$

$$F_C = 40.974 + \left\{\frac{0.160LM - 1.794SM - 1.752AM}{\frac{w}{b}}\right\} \tag{27}$$

3.7.3. Prediction of Fc based on RI, w/b and binder-aggregate ratio (b/agg)

Fig. 10 (a), (b) and (c) displayed the fit regression models of Fc based on the RI, w/b and b/agg for the combination of RM, SM and AM; HM, SM, and AM; and LM, SM and AM respectively. The coefficients of determination (R^2) from Fig. 10 (a), (b) and (c) were 99.64%, 99.64% and 99.66% significantly fit to statistically correlate the data at 95% CI respectively. Also, it was observed that the goodness of fit (R^2 and S) for the prediction of Fc based on RI exhibited the same with the prediction based on both RI and w/b, and RI, w/b and b/agg. This may be as a result of constant w/b and b/agg used during the statistical analysis. Xie and Visintin [16] used a binder-aggregate volume ratio that ranged from 0.045-0.359 and established a significant improvement in the prediction of compressive strength of SCMs blended cement concrete when compared to the use of RI and w/b only [16]. However, it is inferred based on the goodness of fit that the combination of LM, SM, AM, w/b and b/agg yielded the best predictability.

The fit regression equations for the Fc based on RI, w/b and b/agg for the CNSA blended cement concrete at 28 days of curing for M 25 are illustrated in Eqs. 28–30 for the combination of RM, SM, and AM; HM, S, and AM; and LM, SM and AM respectively.

$$F_C = 40.931 + \left\{\frac{0.252RM - 9.220SM - 9.040AM}{\frac{w}{b}}\right\}\left(\frac{b}{agg}\right) \tag{28}$$

$$F_C = 40.993 + \left\{\frac{0.353HM - 9.271SM - 9.040AM}{\frac{w}{b}}\right\}\left(\frac{b}{agg}\right) \tag{29}$$

$$F_C = 40.974 + \left\{\frac{0.827LM - 9.249SM - 9.033AM}{\frac{w}{b}}\right\}\left(\frac{b}{agg}\right) \tag{30}$$

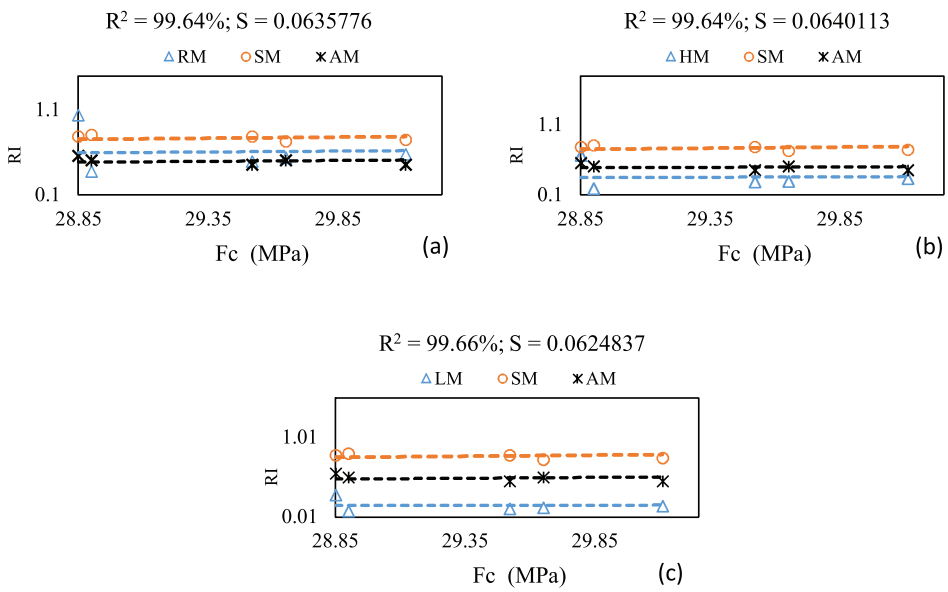

Fig. 10. Fit regression model of Fc based on RI, w/b and b/agg.

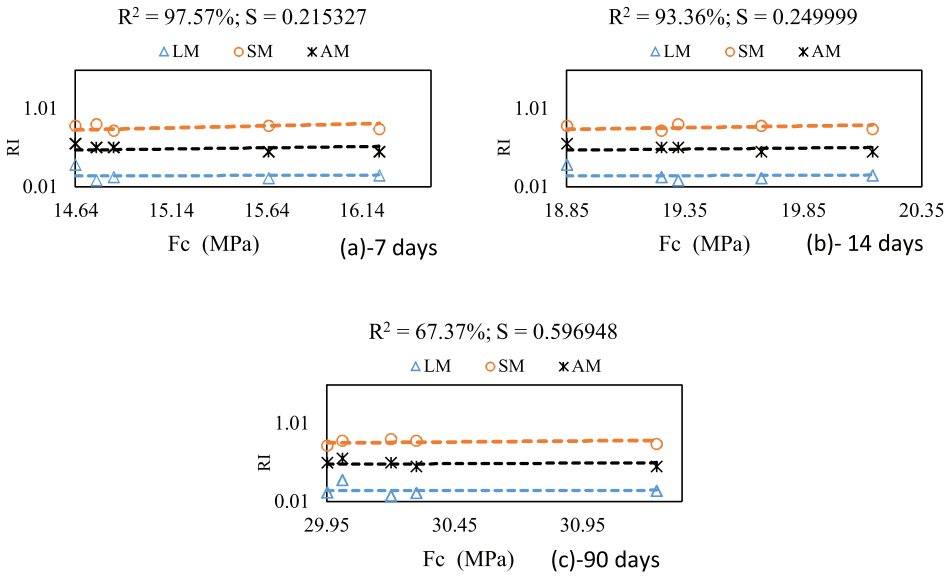

Fig. 11. Fit regression model of Fc over time.

3.7.4. Prediction of Fc over time

The fit regression models in Minitab 17 was also engaged in the prediction of compressive strengths of CNSA blended cement concrete at 7, 14 and 90 days of curing. The best-fit regression models from this study, LM, SM, AM, w/b and b/agg were used to predict the compressive strength and the results are presented in Fig. 11 (a), (b) and (c) for 7, 14 and 90 days of curing respectively. Statistically, it was revealed that the models were 97.57%, 93.36% and 67.37% significantly fit to predict the data at 95% CI for 7, 14 and 90 days of curing respectively.

The fit regression equations for the Fc based on the combination of LM, SM, AM, w/b and b/agg for the CNSA blended cement concrete at 7, 14 and 90 days of curing are illustrated in Eqs. 31–33 for M 25 respectively. Therefore, these developed model equations can be used in the development of mix design of blended concrete as well as a better refinement of existing procedure of concrete mix design provided the chemical composition of the materials is established.

$$F_{C-7\ \text{days}} = 24.630 + \left\{\frac{4.290LM - 0.530SM - 19.230AM}{\frac{w}{b}}\right\}\left(\frac{b}{agg}\right) \tag{31}$$

$$F_{C-14\ \text{days}} = 25.660 + \left\{\frac{0.680LM - 0.790SM - 11.270AM}{\frac{w}{b}}\right\}\left(\frac{b}{agg}\right) \tag{32}$$

$$F_{C-90\ \text{days}} = 36.160 + \left\{\frac{3.020LM - 0.130SM - 12.310AM}{\frac{w}{b}}\right\}\left(\frac{b}{agg}\right) \tag{33}$$

3.7.5. Validation of developed models

The validation of developed regression equations with experimental values and another model equation at 28 days of curing are shown in Fig. 12 (a) and (b) for the Fc based on RI and w/b, and the Fc based on RI, w/b and b/agg respectively. The values of the predicted equations from both figures forecast the same data points and followed the same trend lines with the experimental values. Contrarily, the Xie and Visintin [16]'s model equations forecast a different data point of strengths when compared with both experimental and predicted values. The variation in the validation may be as a result of the difference in chemical and mineralogical compositions of the blended binders, the difference in the type of mix proportion and variation in aggregate used. All these may alter the reactivity and the mechanical properties of the concrete [1,15,16,65,73,75].

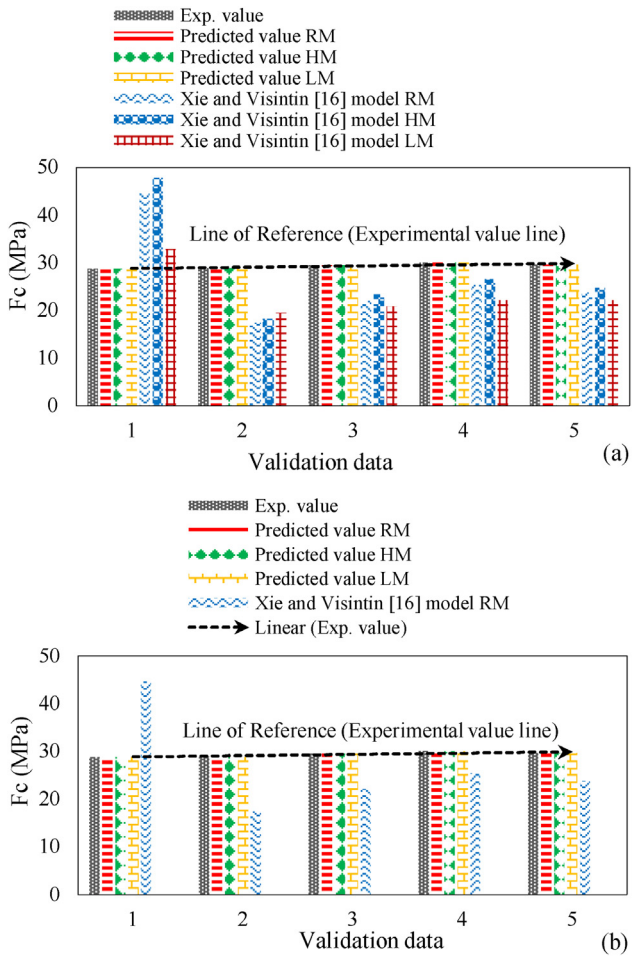

Fig. 12. Validation of developed models at 28 days (a) Fc based on RI and w/b (b) Fc based on R1, w/b, and b/agg.

4. Conclusions

This study evaluated the suitability of CNSA as a supplementary binding material in concrete production. Consequent upon the experimental findings, it can be concluded that CNSA met the requirements of being used as a pozzolanic material in the production of blended cement concrete. Moreover, the workability of freshly mixed concrete increased as the content of CNSA in the mix increased. Furthermore, the mechanical strengths of the concrete increased with increasing CNSA content. In addition, exposure of concrete mixes to an external sulfate attack indicated that concrete incorporated with CNSA exhibited a better resistance than concrete without CNSA to sulfate attack. The micro morphological analysis revealed that the internal pores in the CNSA blended cement mortar reduced with increasing CNSA content in the mix. Finally, an investigation into the RI of binders revealed that the compressive strength of the blended cement concrete can be significantly predicted based on the RI and mix design proportion. Hence, all the developed regression model equations forecast the same data points with the experimental values and these developed model equations can be used in the development of mix design of blended concrete as well as a better refinement of existing procedure of concrete mix design provided the chemical composition of the materials is established. Therefore, this study suggests that a maximum of 15% content of CNSA can be substituted with PLC for structurally applied concrete while 20% can be used for non-load bearing structures. Moreover, the government should put a policy in place that would ensure a full-scale utilization of CNSA in the construction industry. Also, further study should be performed on the long term effect of CNSA on the mechanical and the durability properties of the hardened concrete.

Declaration of Competing Interest

The authors assert that no conflict of interest.

Acknowledgement

The researchers appreciate the Covenant University Centre for Research, Innovation, and Discovery (CUCRID) for the provision of the fund in the course of this study.

References

[1] A.M. Neville, Properties of Concrete, fifth ed., Pearson Education Ltd., England, 2011.
[2] Sustainable Development Goals, Transforming Our World: the 2030 Agenda for Sustainable Development, Report of the United Nations Statistics Division, (2015) . (Accessed 5 April 2019) https://unstats.un.org/sdgs.
[3] A.N. Ede, O. Oshogbunu, O.M. Olofinnade, K.J. Jolayemi, S.O. Oyebisi, O.G. Mark, P.O. Awoyera, Effects of bamboo fibers and limestone powder on fresh properties of self-compacting concrete, 10th Int. Struct. Eng. Constr. Conf. (ISEC-10), Chicago, 2019 ISBN: 978-09960437-6-2.
[4] S. Oyebisi, A. Ede, F. Olutoge, Experimental investigation of 12 molar concentration of activators' salinity on the compressive strength of geopolymer concrete, 4th Int. Sust. Build. Symp. 15 (2019) 191–201, doi:http://dx.doi.org/10.5772/intechopen.87836.
[5] S. Oyebisi, A. Ede, F. Olutoge, O. Ofuyatan, J. Oluwafemi, Modeling of hydrogen potential and strength of geopolymer concrete, Int. J. Civ. Eng. Technol. 9 (7) (2018) 671–679.
[6] S. Oyebisi, A. Ede, F. Olutoge, O. Ofuyatan, J. Oluwafemi, Influence of alkali concentrations on the mechanical properties of geopolymer concrete, Int. J. Civ. Eng. Technol. 9 (8) (2018) 734–743.
[7] S. Oyebisi, A. Ede, O. Ofuyatan, J. Oluwafemi, I. Akinwumi, Comparative study of corncob ash-based lateritic interlocking and sandcrete hollow blocks, Int. J. Geomate 15 (51) (2018) 209–216, doi:http://dx.doi.org/10.21660/2018.51.45918.
[8] A.A. Raheem, S.O. Oyebisi, S.O. Akintayo, M.O. Oyeniran, Effects of admixture on the properties of corncob ash cement concrete, Leonardo Electron, J. Pract. Technol. 16 (2010) 13–20.
[9] O. Ofuyatan, A. Ede, R. Olofinnade, S. Oyebisi, T. Alayande, J. Ogundipe, Assessment of strength properties of cassava peel ash-concrete, Int. J. Civ. Eng. Technol. 9 (1) (2018) 965–974.
[10] S. Oyebisi, A. Ede, F. Olutoge, Predicting the 12 molar concentration of activators' pH and the compressive strength of geopolymer concrete, 4th Int. Sust. Build. Symp. vol.19 (2019) 233–243, doi:http://dx.doi.org/10.5772/intechopen.87836.
[11] S.O. Oyebisi, F.A. Olutoge, M.O. Ofuyatan, A.A. Abioye, Effect of corncob ash blended cement on the properties of lateritic interlocking, Prog. Ind. Ecol. Int. J. 11 (4) (2017) 373–387.
[12] S. Oyebisi, J. Akinmusuru, A. Ede, O. Ofuyatan, G. Mark, J. Oluwafemi, 14 molar concentrations of alkali-activated geopolymer concrete, IOP Conf. Series: Mat. Sci. Eng. vol.413 (2018)012065, doi:http://dx.doi.org/10.1088/1757-899X/413/1/012065.
[13] S. Oyebisi, A. Ede, O. Ofuyatan, T. Alayande, G. Mark, J. Jolayemi, S. Ayegbo, Effects of 12 molar concentration of sodium hydroxide on the compressive strength of geopolymer concrete, IOP Conf. Series: Mat. Sci. Eng. vol. 413 (2018)012066, doi:http://dx.doi.org/10.1088/1757-899X/413/1/012066.
[14] S. Oyebisi, A. Ede, F. Olutoge, O. Ofuyatan, T. Alayande, Building a sustainable world: economy index of geopolymer concrete, 10th Int. Struct. Eng. Constr. Conf. (ISEC-10) (2019) ISBN: 978-0-9960437-6-2.
[15] K.L. Scrivener, R.J. Kirkpatrick, Innovation in use and research on cementitious material, Cem. Concr. Res. 38 (2) (2008), doi:http://dx.doi.org/10.1016/j.cemconres.2007.09.025 128-2008136.
[16] T. Xie, P. Visintin, A unified approach for mix design of concrete containing supplementary cementitious materials based on reactivity moduli, J. Clean. Prod. 203 (2018) 68–82.
[17] T. Xie, T. Ozbakkaloglu, Influence of coal ash properties on compressive behaviour of FA-and BA- based GPC, Mag. Concr. Res. 67 (24) (2015) 1301–1314.
[18] E. Sakai, S. Miyahara, S. Ohsawa, S.H. Lee, M. Daimon, Hydration of fly ash cement, Cem. Concr. Res. 35 (6) (2005) 1135–1140.
[19] İ. Alp, H. Deveci, Y.H. Süngün, A.O. Yilmaz, A. Kesimal, E. Yilmaz, Pozzolanic characteristics of a natural raw material for use in blended cements, Iranian J. Sci. Technol. 33 (2009) 291–300.
[20] E. Aprianti, P. Shafigh, S. Bahri, J.N. Farahani, Supplementary cementitious materials origin from agricultural wastes: a review, Constr. Build. Mater. 74 (2015) 176–187.
[21] N. De Belie, M. Soutsos, E. Gruyaert, Properties of Fresh and Hardened Concrete Containing Supplementary Cementitious Materials: State-of-the-Art Report of the RILEM Technical Committee 238-SCM, Working Group 4, Springer International Publishing, 2017.
[22] B. Lothenbach, K. Scrivener, R. Hooton, Supplementary cementitious materials, Cem. Concr. Res. 41 (12) (2011) 1244–1256.
[23] V. Sata, C. Jaturapitakkul, K. Kiattikomol, Influence of pozzolan from various by-product materials on mechanical properties of high-strength concrete, Constr. Build. Mater. 21 (7) (2007) 1589–1598.
[24] M.M. Johari, J. Brooks, S. Kabir, P. Rivard, Influence of supplementary cementitious materials on engineering properties of high strength concrete, Constr. Build. Mater. 25 (5) (2011) 2639–2648.
[25] A. Fathi, N. Shafiq, M. Nuruddin, A. Elheber, Study the effectiveness of the different pozzolanic material on self-compacting concrete, ARPN J. Eng. Appl. Sci. 8 (2013) 299–305.
[26] V. Ríos-Parada, V.G. Jiménez-Quero, P.L. Valdez-Tamez, P. Montes-García, Characterization and use of an untreated Mexican sugarcane bagasse ash as supplementary material for the preparation of ternary concretes, Constr. Build. Mater. 157 (2017) 83–95.
[27] V.G. Papadakis, S. Tsimas, Supplementary materials in concrete, Part I: Efficiency and design, Cem. Concr. Res. 32 (2002) 1035–1041.
[28] E. Rodriguez-Camacho, R. Uribe-Afif, Importance of using the natural pozzolans on concrete durability, Cem. Concr. Res. 32 (2002) 1851–1858.
[29] F. Massazza, Pozzolanas and durability of concrete, Cem. Concr. World 3 (21) (1999) 19–44.
[30] F. Massazza, Pozzolanic cements, Cem. Concr. Compos. 15 (4) (1993) 185–214.
[31] G. Habert, N. Choupay, J.M. Montel, D. Guillaume, G. Escadeillas, Effects of the secondary minerals of the natural pozzolans on their pozzolanic activity, Cem.Concr. Res. 38 (2008) 963–975.
[32] V.G. Papadakis, S. Antiohos, S. Tsimas, Supplementary materials in concrete. Part II: A fundamental estimation of the efficiency factor, Cem. Concr. Res. 32 (2002) 1533–1538.
[33] S. Antiohos, S. Tsimas, Investigating the role of reactive silica in the hydration mechanisms of high calcium fly ash/cement systems, Cem. Concr. Compos. 27 (2005) 171–181.
[34] F. Seco, L. Ramirez, P. Miqueleiz, B. Urmeneta, E.P. García, V. Oroz, Types of Waste for the Production of Pozzolanic Materials: a Review, (2018) . (accessed 25 May 2019) http://www.intechopen.com.
[35] Food and Agriculture Organization of the United Nations, Food and Agriculture Organization Statistical Pocketbook World Food and Agriculture, (2017) . (accessed 3 November 2018) http://www.fao.org/3/a-i4691e.pdf.
[36] T.F. Akinhanmi, V.N. Atasie, P.O. Akintokun, Chemical composition and physicochemical properties of cashew nut (*Anacardium occidentale*) oil and cashew nut shell liquid, J. Agricul., Food Environ. Sci. 2 (1) (2008) 10–15.
[37] M.B. Ogundiran, J.O. Babayemi, C.G. Nzeribe, Application of waste cashew nut shell ash showed significant reduction in mobility of pb and cd in waste battery contaminated soil, The Pacif. J.Sci. Technol. 12 (2) (2011) 121–126.
[38] K. Pandi, K. Ganesan, Effect of water absorption and sorptivity of concrete with partial replacement of cement by cashew nut shell ash, Austr. J. Basic Appl. Sci. 9 (23) (2015) 311–316.
[39] K. Pandi, R. Anandakumar, K. Ganesan, Study on optimum utilisation of groundnut shell ash and cashew nut shell ash in concrete, Caribb. J. Sci. 53 (1) (2019) 981–991.

[40] V. Thirumurugan1, S.V. George, K. Dheenadhayalan, Experimental study on strength of concrete by partial replacement of cement by cashew nut shell ash and chicken feather fiber as fiber reinforcement, Int. J. Adv. Sci. Res. Dev. 3 (3) (2018) 238–242.
[41] K. Pandi, K. Ganesan, Experimental studies on water absorption and sorptivity of cashew nut shell ash in mortar, Int. J. Acad. Res. Dev. 3 (5) (2018) 151–155.
[42] L.S. Araújo, R.A. João, S.J. Holmer, F. Juliano, Analysis of the cashew nut production waste for use in cement composites, Pro Africa Conf. (2010) 112–119.
[43] Nigerian Industrial Standard 441-1, Industrial Standard Order for Cement Manufacturing, Distribution, Classification and Usage, Nigerian industrial standards, Lagos, Nigeria, 2014.
[44] British Standard EN 196-6, Methods of Testing Cement: Determination of Fineness, BSI, London, 2018.
[45] British Standard EN 12620, Aggregates From Natural Sources for Concrete, BSI, London, 2013.
[46] British Standard 1008, Mixing Water for Concrete: Specification for Sampling, Testing, and Assessing the Suitability of Water, BSI, London, 2002.
[47] M. Behim, M. Beddar, P. Clastres, Reactivity of granulated blast furnace slag, Slovak J. Civ. Eng. 21 (2) (2013) 7–14.
[48] British Standard EN 197-1, Cement: Composition, Specifications and Conformity Criteria for Common Cements, BSI, London, 2016.
[49] British Standard EN 15167-1, Ground Granulated Blast Furnace Slag for Use in Concrete, Mortar and Grout: Definitions, Specifications and Conformity Criteria, BSI, London, 2006.
[50] British Standard EN 206, Concrete Specifications, Performance, Production and Conformity, BSI, 2016.
[51] British Standard EN 12350-2, Testing Fresh Concrete: Method for Determination of Slump, BSI, London, 2009.
[52] British Standard EN 12350-4, Testing Fresh Concrete: Method for Determination of Compacting Factor, BSI, London, 2009.
[53] British Standard EN 12390-3, Testing Hardened Concrete: Compressive Strength of Test Specimens, BSI, London, 2009.
[54] British Standard EN 12390-6, Testing Hardened Concrete: Splitting Tensile Strength of Test Specimens, BSI, London, 2009.
[55] British Standard EN 12390 -5, Testing Hardened Concrete: Flexural Strength of Test Specimens, BSI, London, 2009.
[56] British Standard EN 16523-1, Determination of Material Resistance to Permeation by Chemicals, Under Conditions of Continuous Contact, BSI, London, 2015.
[57] J. Ramonu, J.O. Ilevbaoje, O.A. Olaonipekun, S.O. Oyebisi, O.S. Opeyemi, S. Onikanni, D. Adekunle, S. Abayomi, E. Olumoyewa, Compressive strength analysis of conventional design concrete mix ratio; 1:2:4 and non-conventional concrete mix ratio; 1:3:3 for the construction industry in Nigeria, Int. J. Civ. Eng. Technol. 10 (01) (2019) 1133–1141.
[58] B. Singh, G. Ishwarya, M. Gupta, S.K. Bhattacharyya, Geopolymer concrete: a review of some recent developments, Constr. Build. Mater. 85 (2015) 78–90.
[59] S. Jamkar, C. Rao, Index of aggregate particle shape and texture of coarse aggregate as a parameter for concrete mix proportioning, Cem. Concr. Res. 34 (11) (2004) 2021–2027.
[60] N. Sebaibi, M. Benzerzour, Y. Sebaibi, N.E. Abriak, Composition of self-compacting concrete (SCC) using the compressible packing model, the Chinese method and the European standard, Constr. Build. Mater. 43 (2013) 382–388.
[61] British Standard EN 450-1, Pozzolan for Use in Concrete: Definitions, Specifications and Conformity Criteria, BSI, London, 2012.
[62] American Society for Testing and Materials C 618, Standard Specification for Coal Fly Ash and Raw or Calcined Natural Pozzolan for Use in Concrete, ASTM, 2012.
[63] British Standard EN 8615-2, Specification for Pozzolanic Materials for Use With Portland Cement: High Reactivity Natural Calcined Pozzolana, BSI, London, 2019.
[64] British Standard EN 196-3, Method of Testing Cement: Physical Test, BSI, London, 2016.
[65] N.M. Al Akhras, Durability of metakaolin concrete to sulfate attack, Cem. Concr. Res. 36 (9) (2006) 1727–1734.
[66] British Standard EN 3892-1, Pulverised-fuel Ash: Specification for Pulverised Fuel Ash for Use With Portland Cement, BSI, London, 1997.
[67] K. Celik, C. Meral, A.P. Gursel, P.K. Mehta, A. Horvath, P.J. Monteiro, Mechanical properties, durability, and life-cycle assessment of self-consolidating concrete mixtures made with blended Portland cements containing fly ash and limestone powder, Cem. Concr. Compos. 56 (2015) 59–72.
[68] V. Ríos-Parada, V.G. Jiménez-Quero, P.L. Valdez-Tamez, P. Montes-García, Characterization and use of an untreated Mexican sugarcane bagasse ash as supplementary material for the preparation of ternary concretes, Constr. Build. Mater. 157 (2017) 83–95.
[69] I.I. Akinwumi, O.I. Aidomojie, Effect of corncob ash on the geotechnical properties of lateritic soil stabilized with Portland cement, Int. J. Geomat. Geosci. 5 (3) (2015) 375–392.
[70] F.A. Oluokun, Fly ash concrete mix design and the water-cement ratio law, Mat. J. 91 (1994) 362–371.
[71] W.A. Gutteridge, J.A. Dalziel, Filler cement: the effect of the secondary component on the hydration of Portland cement, Part I. A fine non-hydraulic filler, Cem. Concr. Res. 20 (1990) 778–782.
[72] M. Cyr, P. Lawrence, E. Ringtot, Mineral admixtures in mortars: quantification of the physical effect of inert materials on short-term hydration, Cem. Concr. Res. 35 (2005) 719–730.
[73] J. Skibsted, R. Snellings, Reactivity of supplementary cementitious materials (SCMs) in cement blends, Cem. Concr. Res. 124 (2019)105799.
[74] J.W. Bullard, E.J. Garboczi, P.E. Stutzman, P. Feng, A.S. Brand, L. Perry, J. Hagedorn, W. Griffin, J.E. Terril, Measurement and modelling needs for microstructure and reactivity of next-generation concrete binders, Cem. Concr. Compos. 101 (2019) 24–31.
[75] K.L. Scrivener, B. Lothenbach, N. de Belie, E. Gruyaert, J. Skibsted, R. Snellings, A. Vollpracht, Hydration and microstructure of concrete with SCMs: state of the art on methods to determined degree of reaction of SCMs, Mater. Struc. 48 (2015) 835–862.
[76] J. Kamaul, A. Ahmed, P. Hirst, J. Kangwa, Suitability of corncob ash as a supplementary cementitious material, Int. J. Mat. Sci. Eng. 4 (4) (2016) 215–228.
[77] F. Tu rker, F. Akoz, S. Koral, N. Yuzer, Effects of magnesium sulfate concentration on the sulfate resistance of mortars with and without silica fume, Cem. Concr. Res. 27 (1997) 205–214.
[78] A. Al Salami, A. Salem, Effects of mix composition on the sulfate resistance of blended cements, Int. J. Civ. Struct. Environ. Infrastruct. Eng. Res. Dev. 10 (6) (2010) 37–41.
[79] H.Y. Moon, T. Lee, S. Kim, Sulphate resistance of silica fume blended mortars exposed to various sulphate solutions, Canad. J. Civ. Eng. 30 (2003) 625–636.
[80] V.M. Malhotra, M.H. Zhang, P.H. Read, J. Ryell, Long-term mechanical properties and durability characteristics of high-strength/high-performance concrete incorporating supplementary cementing materials under outdoor exposure conditions, Mater. J. 97 (5) (2000) 518–525.
[81] J.D. Bapat, Mineral Admixtures in Cement and Concrete, first ed., CRC Press, Boca Raton, 2012.
[82] J. Tishmack, J. Olek, S. Diamond, Characterization of high calcium fly ashes and their potential influence on ettringite formation in cementitious systems, Cem. Concr. Aggreg. 21 (1999) 82–92.
[83] Q. Wang, D. Wang, H. Chen, The role of fly ash microsphere in the microstructure and macroscopic properties of high-strength concrete, Cem. Concr. Compos. 83 (2017) 125–137.
[84] A.K.H. Kwan, Y. Li, Effects of fly ash microsphere on rheology, adhesiveness and strength of mortar, Constr. Build. Mater. 42 (2013) 137–145.
[85] Y. Li, A.K.H. Kwan, Ternary blending of cement with fly ash microsphere and condensed silica fume to improve the performance of mortar, Cem. Concr. Compos. 49 (2014) 26–35.
[86] L. Guangwei, Z. Huajun, Z. Zuhua, W. Qisheng, Effect of rice husk ash addition on the compressive strength and thermal stability of metakaolin based geopolymer, Constr. Build. Mater. 22 (2019) 872–881.
[87] M. Mehdi, S. Yasser, Thermal and microstructure properties of cement mortar containing ceramic waste powder as alternative cementitious materials, Constr. Build. Mater. 223 (2019) 643–656.